Article

Not peer-reviewed version

Enhanced Electrochemical Performance of La0.7Pr0.3Ba0.5Sr0.5Co1.5Fe0.5O5+δ Cathodes for Solid Oxide Fuel Cells by La2NiO4 impregnation

Chengcheng Wang *, Zhanggui Li, Zhiheng Zheng, Jianyi Zhong, Jiali Xiang, Rui Wang, Bingxue Hou, Zanxiong Tan, Xintao Wang

Posted Date: 7 June 2024

doi: 10.20944/preprints202406.0496.v1

Keywords: Solid oxide fuel cell; solution impregnation technique; La1-xPrxBa0.5Sr0.5Co1.5Fe0.5O5+δ(LPBSCF)

Article

Enhanced Electrochemical Performance of $La_{0.7}Pr_{0.3}Ba_{0.5}Sr_{0.5}Co_{1.5}Fe_{0.5}O_{5+\delta}$ Cathodes for Solid Oxide Fuel Cells by La_2NiO_4 Impregnation

Cheng Cheng Wang [1,3,*], Zhanggui Li [1,3], Ziheng Zheng [1], Jianyi Zhong [1], Jiali Xiang [1], Rui Wang [1], Bingxue Hou [2], Zanxiong Tan [1] and Xintao Wang [1,*]

[1] Shen Zhen Polytechnic University, Shenzhen, 518055, China
[2] Aviation Engineering Institute, Civil Aviation Flight University of China, GuangHan,618037, China
[3] The authors are making the same contribution to the paper.
* Correspondence: wangchengcheng@szpt.edu.cn (C.C.W.); wangxintao@szpt.edu.an (X.W.)

Abstract: Three types of double perovskite $La_{1-x}Pr_xBa_{0.5}Sr_{0.5}Co_{1.5}Fe_{0.5}O_{5+\delta}$(x=1,0.3,0) are prepared using the EDTA-citrate method and identified as solid oxide fuel cell (SOFC) cathodes. The microstructures, as well as electrochemical performances of $La_{1-x}Pr_xBa_{0.5}Sr_{0.5}Co_{1.5}Fe_{0.5}O_{5+\delta}$ (LPBSCF) and La_2NiO_4-impregnated LPBSCF (LN-LPBSCF) cathodes, are investigated in detail. An optimum impregnation amount of LN-LPBSCF (LN loading of 0.64 mg/cm^2) electrode exhibits relatively lower electrode polarization resistance (Rp) and better stable performance as compared to that of pure LPBSCF electrode in symmetrical SOFCs. The maximum power density of LN-LPBSCF single cells is 800 mW/cm^2 at 800 °C and demonstrates good stability for 100 h in short-term testing.

Keywords: Solid oxide fuel cell; solution impregnation technique; $La_{1-x}Pr_xBa_{0.5}Sr_{0.5}Co_{1.5}Fe_{0.5}O_{5+\delta}$(LPBSCF)

1. Introduction

Recent years, renewable energy techniques have attracted more attention because of classical fuel resources declining and concerns over environmental pollution. IT-SOFCs operating at 600-800 °C are of great interests due to fuel flexibility and appropriate for a great variety of applications [1–4]. However, one of the greatest difficulties by choosing an appropriate cathode material is because of the increased Rp and poor ORR activity [5,6]. Nowadays, many researchers are paying more attention to develop mixed ionic-electronic conductors (MIECs).

Due to layered structure, lower polarization resistances and higher catalytic activities of double perovskite (DP) and Ruddlesden-Popper (RP) , they are widely investigated as cathode materials for IT-SOFCs [7–11]. Cation-ordered $LnBaCo_2O_{5+d}$ oxides have been paid more attention due to faster oxygen ion diffusion and higher electrical conductivity [12–14]. Shao Z.P. et al. [15] ever did a systematic study of $PrBaCo_2O_{5+\delta}$ + $Sm_{0.2}Ce_{0.8}O_{1.9}$ composites as electrodes of SOFC, in which reckoned that improved performance of 70 wt% PBC+30 wt% SDC was due to a reduction of oxygen-ions diffusion path. Moreover, Wang H.R. et al. [16] recently studied that $PrBaCo_2O_{5+d}$ (PBC)+ $NdMnO_3$ composite cathode in reversible solid oxide cells, and got the conclusion that PBC-$NdMnO_3$ (NM) composites showed good electrochemical performances and reversible cycle performance. Furthermore, Sr and Fe doping in $PrBaCo_2O_{5+d}$ enhanced thermal expansion behavior and ORR activity [17]. Wang S.R. et al.[17] recently studied that maxmium power density of $PrBa_{0.5}Sr_{0.5}Co_{1.5}Fe_{0.5}O_{5+\delta}$ (PBSCF) | $BaZr_{0.1}Ce_{0.7}Y_{0.1}Yb_{0.1}O_{3-\delta}$ (BZCYYb) | NiO-BZCYYb | NiO-BZCYYb single cell at 750 °C was 958.75 mW cm^{-2} using dry H_2 as fuel.

Solution impregnation technique is one of the widely used techniques to prepare nano-structured SOFC cathodes with good electrochemical performance [18–26]. There are several reports available on application of solution impregnation of SOFC cathodes. Li J. et al. [6] ever did a

 doi:10.20944/preprints202406.0496.v1

systematic research on the electrochemical performance of La_2NiO_4-impregnated PBSCF cathode for SOFC, and they got the conclusion that PBSCF with LN impregnation of an average thickness (9 nm) showed lowest initial polarization resistance of 0.51 Ω cm^2 and highest power density of 0.71 W/cm^2 . They also reckoned that LN had higher oxygen surface exchange coefficient and LN coating depressed Sr segregation . Chen K.F. et al. ever reported that a BaO infiltrated LSCF exhibited better tolerance and resistance towards Cr poisoning due to preventing excess Sr deficiency at the A-site of LSCF and thus preventing Cr poisoning effect [27]. Huang J.Y. et al. recently reported that infiltration of $BaCO_3$ into LSCF could increase the performance of the single cell and it could deliver a peak power density of 1.30 W cm^{-2} at 800 °C [28].

To make better usage of DP and RP, RP-impregnated DP cathode was investigated by solution impregnation in the present study. The effect of LN impregnation on the electrochemical performances of $La_{1-x}Pr_xBa_{0.5}Sr_{0.5}Co_{1.5}Fe_{0.5}O_{5+\delta}$(LPBSCF, x=0.3) electrode was investigated. Moreover, the effect of different impregnation loadings of LN was simultaneously studied under SOFC operating conditions. Results clearly showed that impregnation LN can decrease electrode polarization resistance of $La_{1-x}Pr_xBa_{0.5}Sr_{0.5}Co_{1.5}Fe_{0.5}O_{5+\delta}$(LPBSCF, x=0.3) cathodes and increased single cell stability.

2. Experimental

2.1. Powder Preparation

A series of $La_{1-x}Pr_xBa_{0.5}Sr_{0.5}Co_{1.5}Fe_{0.5}O_{5+\delta}$ (x=1,0.3,0) were synthesized using the traditional sol–gel method. Firstly, all metal nitrates (La, Pr, Ba, Sr, Co, and Fe) (Sigma Corporation,99.9% trace metal basis) were weighed and dissolved in distilled water at stoichiometric ratios. Secondly, citrate acid (CA) (n(metal cations):n(CA)=1:1.5) was added to the solution, while ethylenediaminetetraacetic acid (EDTA) (n(metal cations):n(EDTA)=1:1) was mixed with $NH_3.H_2O$ and stirred at 80 °C for 4 h. Finally, three types of powders were sintered at 900, 950, and 1000 °C for 4 h to identify the crystalline phase formation.

2.2. Symmetrical Half-Cells and Single Cells Fabrication

The procedure for making symmetrical cells was as follows: a dense $Gd_{0.1}Ce_{0.9}O_{1.95}$(GDC) electrolyte disc pellet with a diameter of Φ16 mm was obtained from Handan Technology Co. $La_{1-x}Pr_xBa_{0.5}Sr_{0.5}Co_{1.5}Fe_{0.5}O_{5+\delta}$ (LPBSCF) (x=1,0.3,0) powder was mixed with terpineol solvents and ethyl cellulose binders to create uniform cathode slurries. These slurries were then screen-printed on both sides of the GDC pellet and sintered at 1050 °C for 3 h to form uniform LPBSCF cathodes.

$La(NO_3)_3$ and $Ni(NO_3)_2$ solution (0.08 mol/L; Aladdin Industrial Corporation) were infiltrated into LPBSCF(x=0.3) cathodes and fired at 950 °C for 2 h. Each side of La_2NiO_4 loading was 0.64 and 1.28 mg/cm^2 (referred to as LPBSCF3-LN-0.04M and LPBSCF3-LN-0.08M, respectively). Pt paste was applied onto the surface of the LPBSCF-LN electrode as a current collector and heated in an oven at 200 °C for 2 h. A silver paste was used to connect the wires. LN solution was dried and calcined in air at 950 °C for 2 h to form LN powder for phase identification. The chemical compatibility of LPBSCF(x=0.3) and LN powders was confirmed at 1000 °C for 3 h.

Commercial SOFC button half-cells (NiO-YSZ|YSZ|GDC) with a diameter of Φ16 mm (Ningbo Qingbang Company) were obtained for performance testing. The cathode slurry was applied onto the GDC layer (surface area of 0.2826 cm^2) and fired at 1050 °C for 3 h. The impregnation and sintering methods for LPBSCF3-LN-0.04M were the same as those for the symmetrical cell mentioned above.

 doi:10.20944/preprints202406.0496.v1

2.3. Electrochemical and Microstructural Characterization

The electrochemical performances of LPBSCF and LN-LPBSCF cathodes were evaluated using the three-electrode method at 700 °C, employing an electrochemical workstation (Shanghai Chenhua). The potential at a cathodic current of 200 mA cm^{-2} was recorded at 700 °C for 40 h. Electrochemical impedance spectroscopy (EIS) curves were collected under open circuit voltage (OCV) conditions (0.1 Hz to 100 kHz) with a signal amplitude of 10 mV. Rp was obtained from the difference between the high- and low-frequency intercepts. The current (I)-voltage (V) and current (I)-power (P) of single-cells were obtained using hydrogen (3% H_2O/97% H_2) fuel (Corrtest CS, Wuhan CorrTest Instruments Corp., Ltd.) with a flow rate of 40 mL/min at 800 °C.

The phase formation and chemical compatibility of the powders were tested by X-Ray diffraction (XRD; Bruker, D8 Advances) from 10° to 80° (2θ). Scanning electron microscopy (SEM, ZEISS) and transmission electron microscopy (TEM, Titan G2 60-300) were used to examine the powder morphology. The surfaces and cross-sections of the LPBSCF3, LPBSCF3-LN-0.04M, and LPBSCF3-LN-0.08M cathodes and single cells were examined using SEM (NEON 40ESB) and energy dispersive spectroscopy (EDS). Focused ion beam scanning electron microscopy (FIB-SEM, Helios G4 PFIB, CXe DualBeam) was used to characterize the microstructure and elemental mapping of a typical cross-section of the LPBSCF3-LN-0.04M cathode.

3. Results and Discussion

Figure 1(a–c) illustrates the XRD patterns for $La_{1-x}Pr_xBa_{0.5}Sr_{0.5}Co_{1.5}Fe_{0.5}O_{5+\delta}$ (LPBSCF) (x=1,0.3,0) powders firing at different temperatures (900–1000 °C). No impurity phase was observed when sol–gel was fired at 1000 °C for all powders. As shown in Fig. 1b, a small peak was obtained at approximately 30° when LPBSCF(x=0.3) was fired at 900 °C, which was related to $SrFeO_4$ with JCPDS of 29-1305. Two peaks were also obtained when LPBSCF(x=0) was fired at 900 and 950 °C, correlating to $BaFe_2O_4$ with JCPDS of 26-0158 by Jade software. The pure phase LPBSCF(x=1,0.3,0) was obtained by the EDTA-citrate method at 1000 °C.

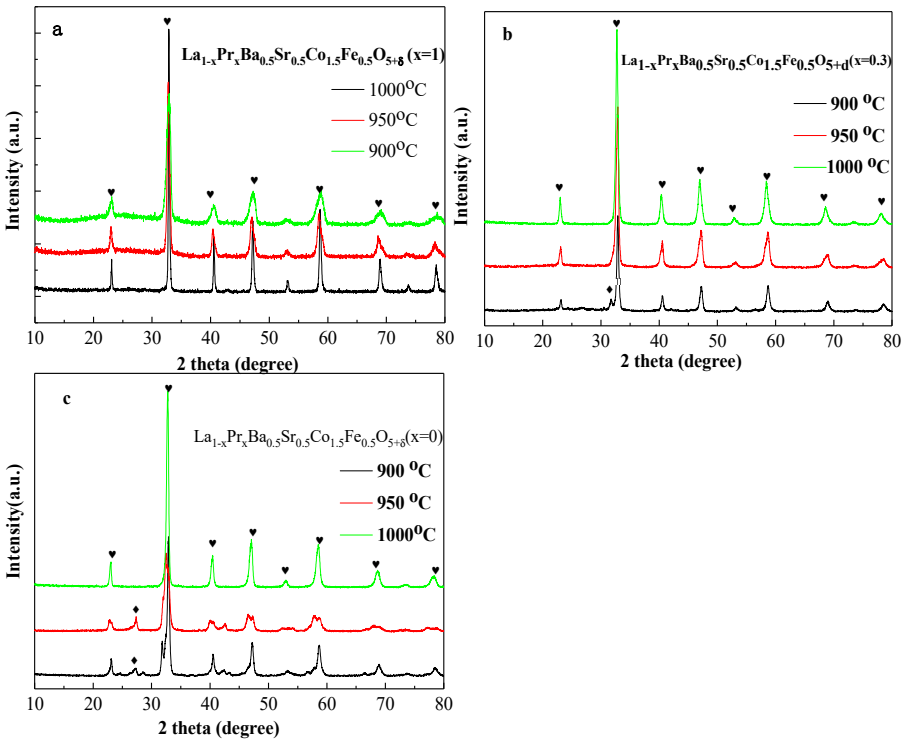

Figure 1. XRD of $La_{1-x}Pr_xBa_{0.5}Sr_{0.5}Co_{1.5}Fe_{0.5}O_{5+\delta}$ (x=1, 0.3 and 0) powders calcined at 900, 950 and 1000 °C for 3 h in air. a:x=1,b:x=0.3,c:x=0.

 doi:10.20944/preprints202406.0496.v1

To identify powder morphology, Fig. 2a shows that LPBSCF(x=1) particles firing at 1000 °C were dispersed, with some irregular particles (at approximately 30–200 nm). The inset of Fig. 2a shows that the EDX spectrum contains only the Pr, Ba, Sr, Co, Fe, and O spectra. According to the quantitative EDS results, the atomic ratios of Pa, Ba, Sr, Co, Fe, and O were 8.46%, 4.93%, 5.76%, 13.98%, 4.77%, and 62.09%, respectively. Figure 2b shows that the average size of the LBSCF (x=0.3) was approximately 200 nm, and compared to that of Fig. 2a, the particles were more uniform in shape. According to the EDS results, the atomic ratios of La, Pr, Ba, Sr, Co, Fe, and O were 6.05%, 2.45%, 4.63%, 5.26%,12.84%, 4.27%, and 64.51%, respectively. Moreover, the LPBSCF(x=0) particles were well distributed and connected, as shown in Figure 2c. The average particle size was approximately 220 nm.

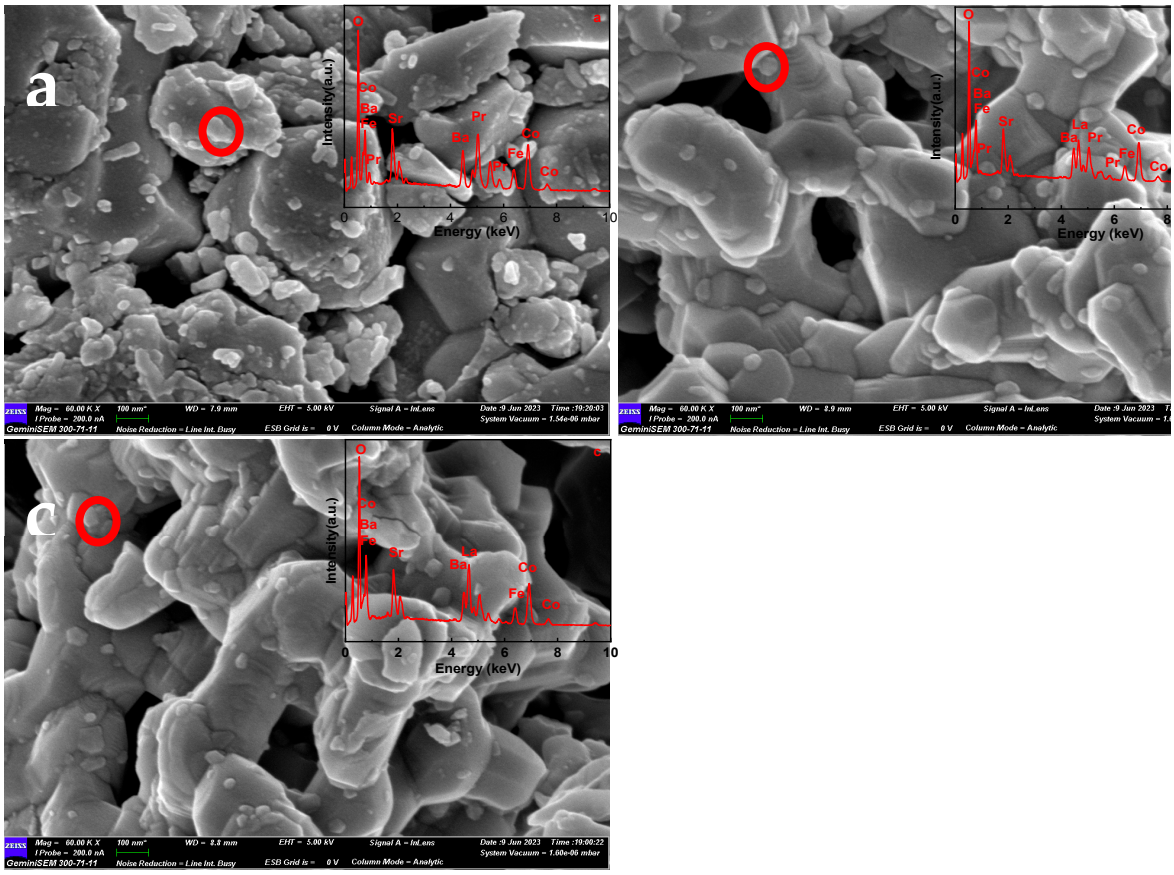

Figure 2. SEM images for $La_{1-x}Pr_xBa_{0.5}Sr_{0.5}Co_{1.5}Fe_{0.5}O_{5+\delta}$(LPBSCF) (x=1, 0.3 and 0) powders fired at 1000 °C for 3 h in air and EDS spectra of powders.

In order to test the impedance of LPBSCF electrode at lower temperature, the initial EIS of three LPBSCF (x=1,0.3,0) cathodes firing at 1000 °C were acquired in air at 700 °C under open circuit condition (Figure 3a–c). The R_P of LPBSCF (x=0.3) was 0.5 cm^2, which was lower than that of LPBSCF (x=1, 0), and the Rp values of LPBSCF(x=0.3) were smaller than those in previous studies [6], which might indicate that the interface of the cathode and electrolyte connected well with each other. Deconvoluting EIS at 700 °C into R_{PH} and R_{PL} were obtained, which are listed in Table 1. LPBSCF (x=0.3) exhibited a relatively lower R_{PL} than LPBSCF(x=1,0), indicating that the surface reaction products were relatively easily transported away from the surface [6].

Preprints.org (www.preprints.org) | NOT PEER-REVIEWED | Posted: 7 June 2024 doi:10.20944/preprints202406.0496.v1

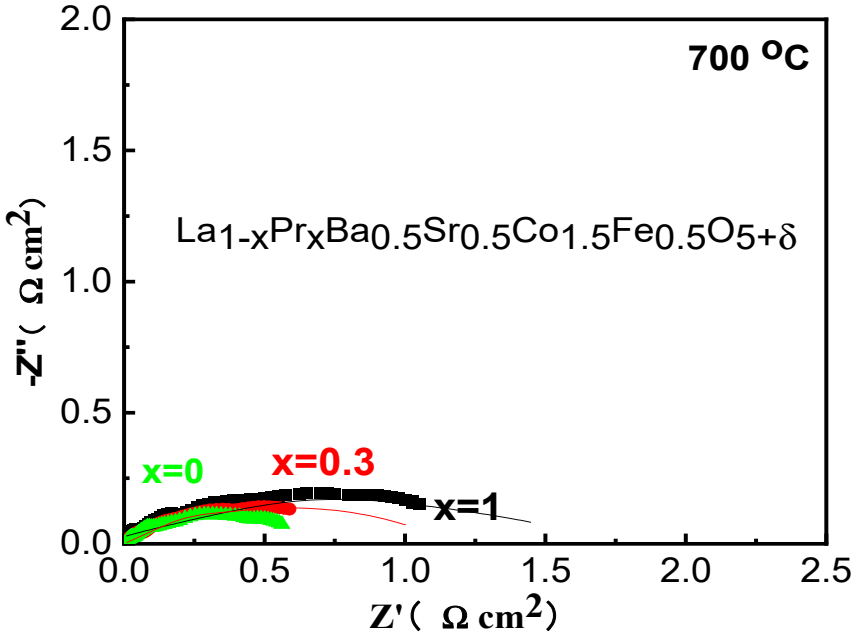

Figure 3. Electrochemical impedance spectra acquired with $La_{1-x}Pr_xBa_{0.5}Sr_{0.5}Co_{1.5}Fe_{0.5}O_{5+\delta}$ (x=1, 0.3 and 0) cathodes measured at 700 °C in air. The insert is the equivalent circuit for data fitting.

Table 1. Polarization resistances of prepared $La_{1-x}Pr_xBa_{0.5}Sr_{0.5}Co_{1.5}Fe_{0.5}O_{5+\delta}$ (x=1, 0.3 and 0) cathodes under open circuit condition at 700 °C.

700 °C Stable 2h	LPBSCF(x=1)	LPBSCF(x=0.3)	LPBSCF(x=0)
$R_P/\Omega\cdot cm^2$	1.2	0.5	0.6
$R_{PH}/\Omega\cdot cm^2$	0.1	0.1	0.1
$R_{PL}/\Omega\cdot cm^2$	1.1	0.4	0.5

In this study, pure phase La_2NiO_4 (LN) was obtained using the EDTA-citrate method, as shown in Figure 4a. To confirm the chemical compatibility of LN and LPBSCF(x=0.3), these powders were co-fired at 1000 °C for 3 h. According to the results shown in Figure 4b, all powders formed a pure phase with their crystal plane index, and no other impurity peaks were observed. The crystal plane index was determined based on previous studies [29,30]. Figure 5 shows the cross-sectional SEM images of the LPBSCF3, LPBSCF3-LN-0.04M, and LPBSCF3-LN-0.08M electrodes before the electrochemical tests. The size of the LPBSCF3 particles had a width size of 0.5–1 μm. The surfaces were smooth, and the distribution of different pores was uniform (Figure 5a,b). After impregnation with LN 0.04 M and 0.08 M (Figs. 5c,d and e,f, respectively), there were significant microstructural changes. The surfaces of the LPBSCF3 particles were rough, and more needle-like particles were observed (Figure 5c,e). More needle-like particles are depicted in Figure 5e compared to Figure 5c, indicating that more LN particles covered the surface of the LPBSCF3 particles. Moreover, according to the SEM results, the porosity of LPBSCF3-LN-0.04M and LPBSCF3-LN-0.08M were less than that of LPBSCF3.

 doi:10.20944/preprints202406.0496.v1

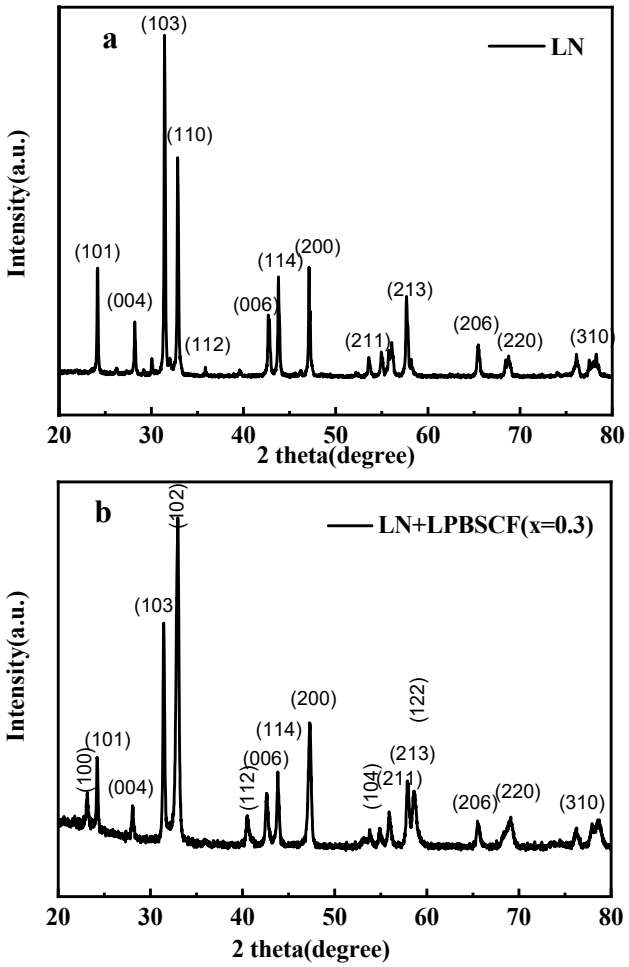

Figure 4. XRD of La_2NiO_4 (LN) powders fired from its nitrates solution calcined at 1000 °C for 3 h (a), and XRD pattern of $La_{1-x}Pr_xBa_{0.5}Sr_{0.5}Co_{1.5}Fe_{0.5}O_{5+\delta}$ (x=0.3, LPBSCF3) and LN powders' compatibility test (b).

To identify the internal cross-sectional microstructure of the LPBSCF3-LN-0.04M cathodes. Figure 6 shows a cross-sectional image of the LPBSCF3-LN-0.04M cathode obtained by FIB-SEM. Figure 6a shows the internal width of the cathode, which is approximately 12.80 um. The pores were homogeneously distributed in the bulk of the cathode. Moreover, needle-like particles were located inside the LPBSCF3 cathode, detected within the electrode bulk, and their size was approximately 100 nm (Figure 6b,c). EDS analysis illustrates the presence of La and Ni, as well as Pr, Ba, Sr, Co, Fe, and O, as shown in Figure 6d.

 doi:10.20944/preprints202406.0496.v1

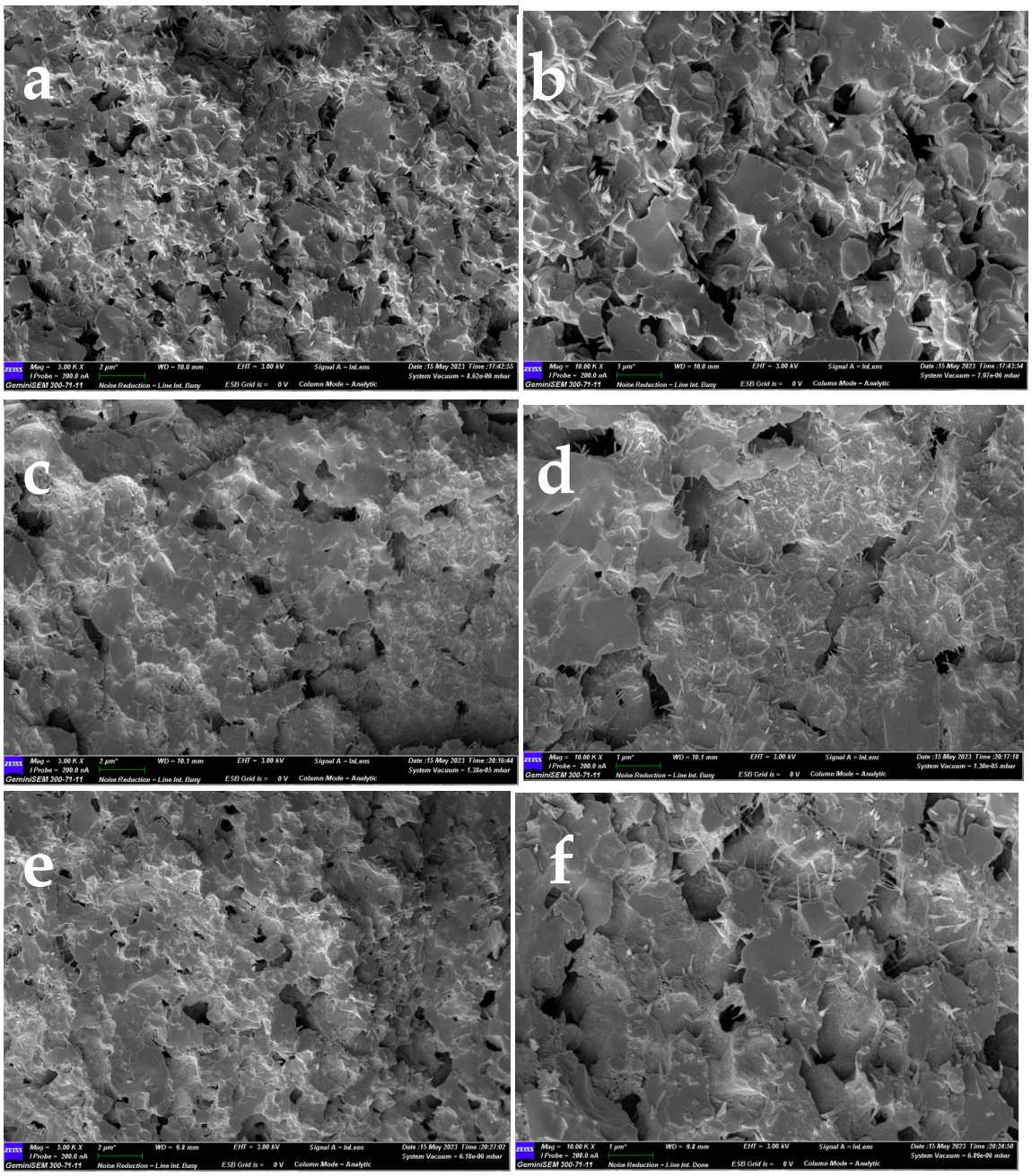

Figure 5. Cross-sectional micro structures of (a) LPBSCF3 cathode; (b) impregnated LPBSCF3-LN-0.04M cathode; (c) impregnated LPBSCF3-LN-0.08M cathode.

 doi:10.20944/preprints202406.0496.v1

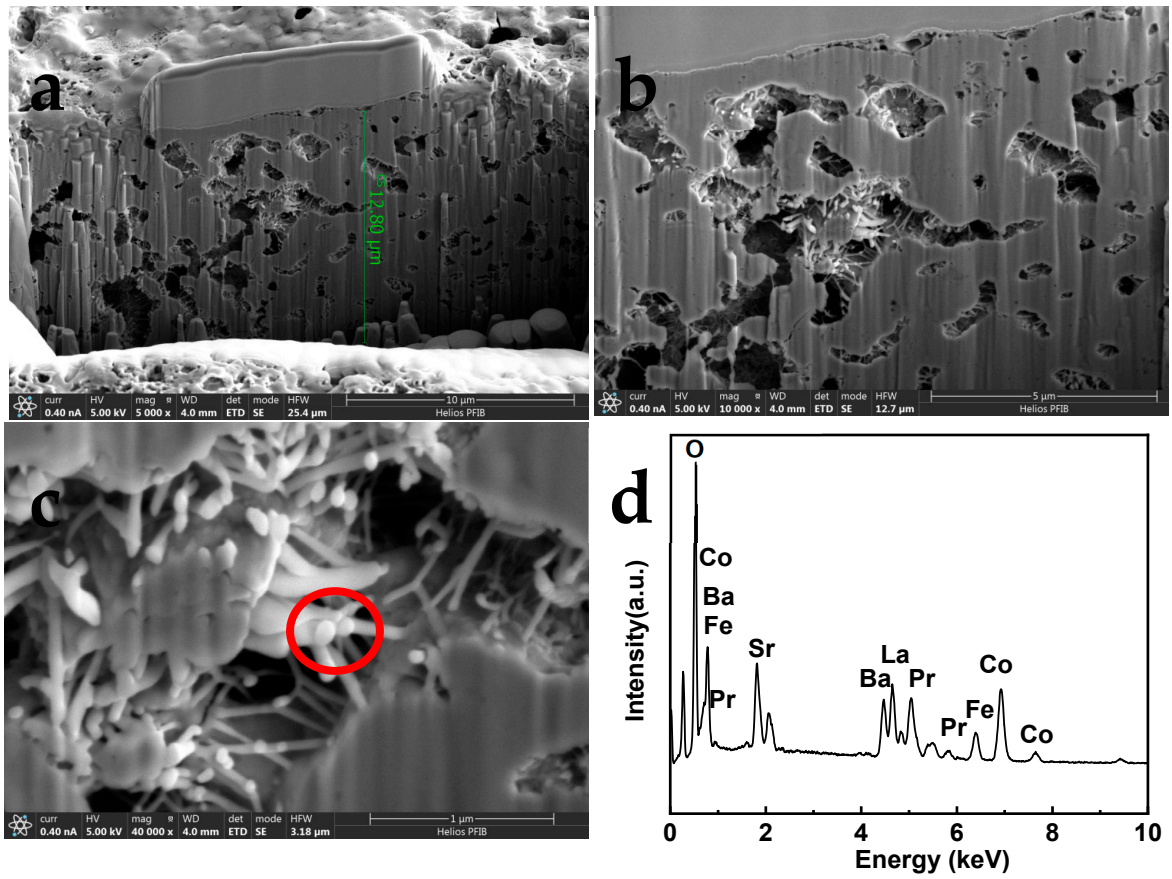

Figure 6. FIB-SEM of cross-section micro structures of impregnated LPBSCF3-LN-0.04M cathode.

To identify the needle-like particles, the LPBSCF3-LN-0.04M cathodes were peeled directly from the symmetrical cell. Figure 7 shows the TEM and EDS elemental maps of the LPBSCF3-LN-0.04M cathodes. Notably, a very thin layer covered the top of the LPBSCF3 particles, with an average thickness of approximately 6 nm. However, according to the EDS mapping results, it cannot be concluded that the composition of the thin layer is LN, which differs from what has been previously reported regarding the formation of the core-shell structure of LN-PBSCF cathodes From our perspective, this could be owing to the different preparation procedures using different solvents and surfactants.

 doi:10.20944/preprints202406.0496.v1

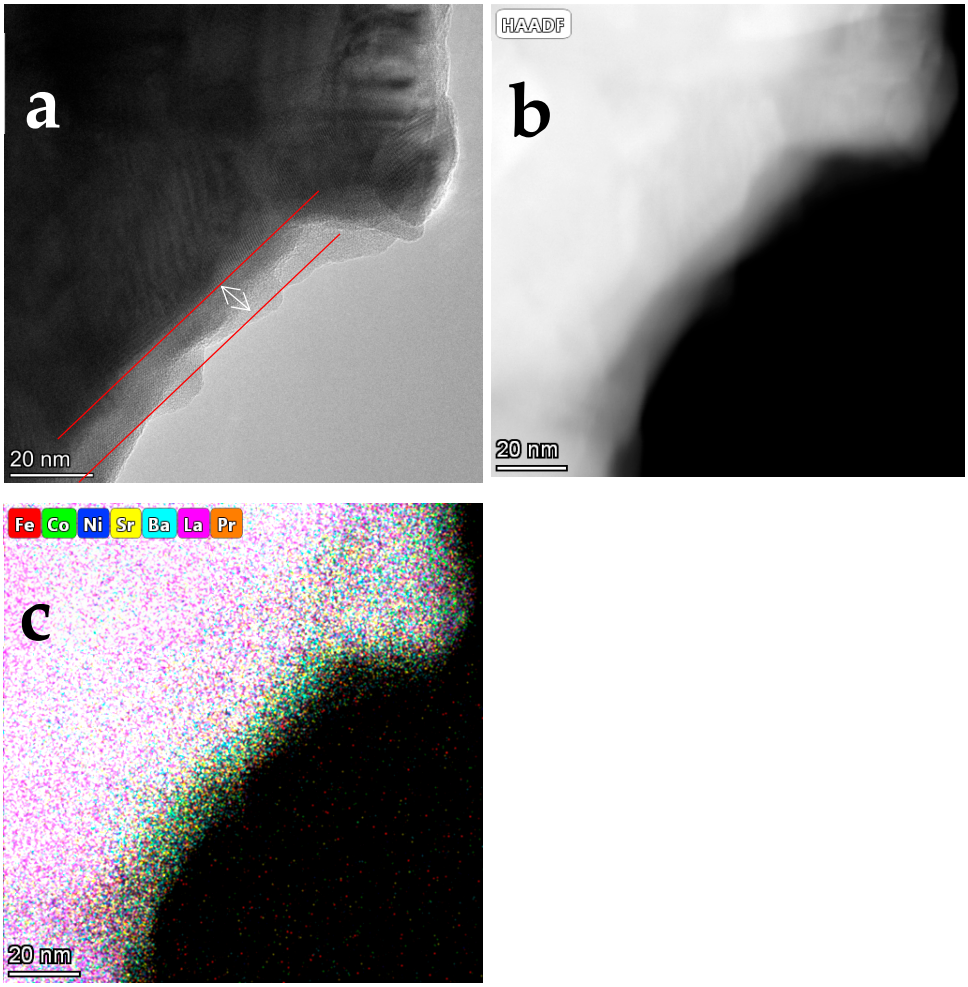

Figure 7. TEM of impregnated LPBSCF3-LN-0.04M cathode under high magnifications.

The stability of the electrochemical performances of the cathodes was assessed through EIS under cathodic current polarization at 200 mA/cm^2 at 700 °C for 40 h, as shown in Figure 8. The obtained R_{PH} and R_{PL} values are listed in Table 2. Notably, R_P for LPBSCF3 was 0.6 Ωcm^2, which was the lowest among those for LPBSCF3-LN-0.04M(0.7 Ωcm^2) and LPBSCF3-LN-0.08M (1.2 Ωcm^2). The R_P of low LN impregnation loading-LPBSCF3 was similar to that of LPBSCF3; however, a higher impregnation of LN in LPBSCF3-LN-0.08M compromised its benefit. Impregnation LPBSCF with the appropriate amount of LN (high k*~10^{-6} cm s^{-1} at 590 °C) [31] could promote oxygen adsorption-dissociation processes and create more O^{2-} on the cathode surface. However, this study showed that a higher impregnation LN (0.08M) prevented surface O^{2-} from being transported quickly into the cathode bulk due to low D* for LN (10^{-8} cm^2 s^{-1} for LN) [32], therefore, LPBSCF3-LN-0.04M demonstrated a relatively lower value of R_{PL} and R_P. Moreover, they all then increased to some values after approximately 40 h. By calculating the increase ratio of Rp from t=2 h to t=40 h, LPBSCF3-LN-0.04M exhibited a relatively lower increase of Rp over time due to the increase in polarization time. These results indicate that by optimizing the impregnation loading amount of LN and utilizing the synergistic effect of LN and LPBSCF, LPBSCF3-LN-0.04M cathodes could demonstrate a relatively stable performance against current polarization compared to the LPBSCF3 and LPBSCF3-LN-0.08M cathodes.

 doi:10.20944/preprints202406.0496.v1

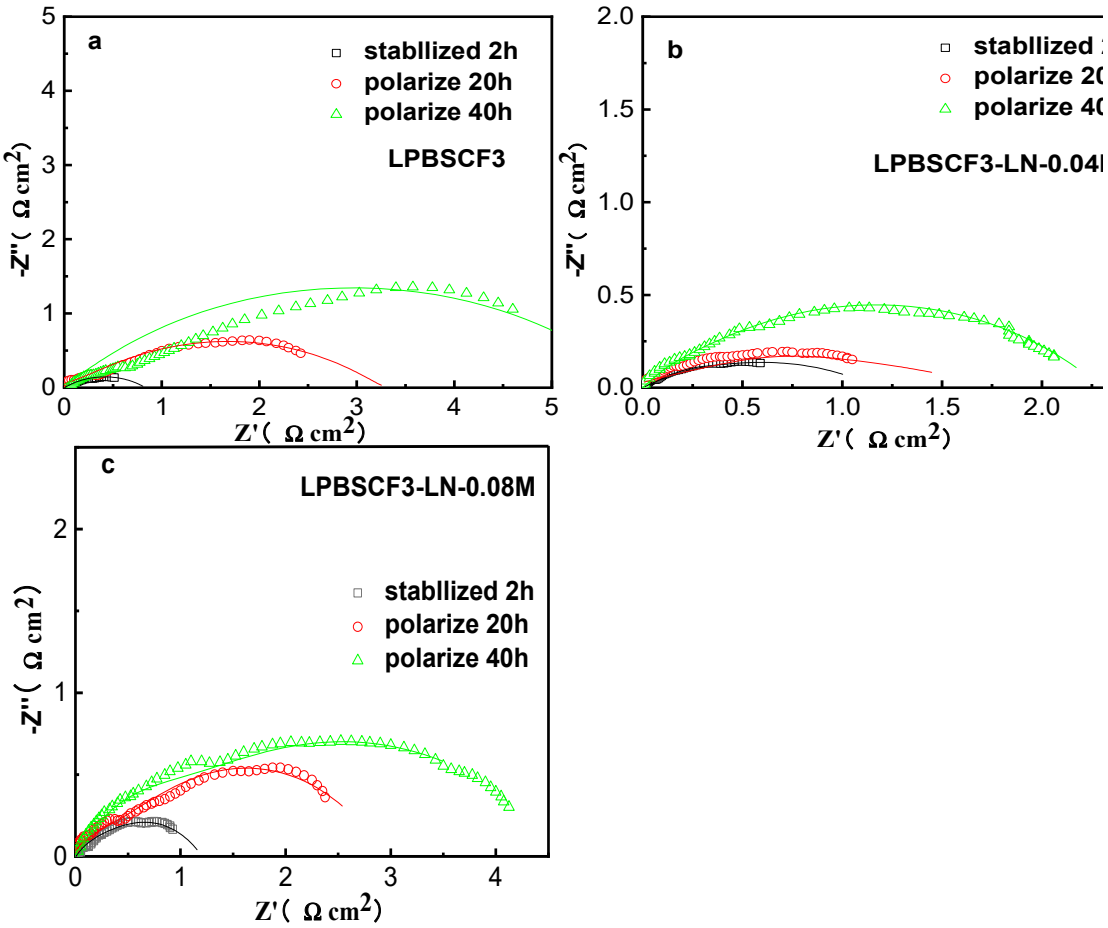

Figure 8. Electrochemical impedance spectra of LPBSCF3 (a) and impregnated LPBSCF3-LN-0.04M (b), impregnated LPBSCF3-LN-0.08 M (c) cathodes using Ag as collectors, and polarization resistances of these three cathodes as a function of temperature (d) at a constant current density of 200 mA/cm^2 at 700 ^{o}C for 40 h in symmetrical cells.

Table 2. Summarized polarization resistances of prepared LPBSCF (x= 0.3),LPBSCF(x=0.3)-LN-0.04 M and LPBSCF(x=0.3)-LN-0.08 M cathodes before and after cathodic current of 200 mA/cm^2 at 700 ^{o}C for 40 h.

0mA/cm^2	**LPBSCF3 Stable 2h**		**LPBSCF3-LN-0.04M Stable 2h**		**LPBSCF3-LN-0.08 M Stable 2h**	
R_P	0.6		0.7		1.2	
R_{PH}	0.1		0.1		0.1	
R_{PL}	0.5		0.6		1.1	
200mA/cm^2	20h	40h	20h	40h	20h	40h
R_P	2.7	5	1.2	2.2	2.5	4.3
R_{PH}	0.2	0.3	0.2	0.1	0.2	0.2
R_{PL}	2.5	4.8	1.0	2.1	2.3	4.1

Figure 9 shows the cross-sectional SEM images of the LPBSCF3, LPBSCF3-LN-0.04M, and LPBSCF3-LN-0.08M electrodes after electrochemical tests. As shown in Figure 9c, there was a good connection between LPBSCF3-LN-0.04M and GDC. Compared with Figure 5, there were significant microstructural changes after the tests. No needle-like particles were observed in Figs. 9d and 9f. Moreover, the cathode surfaces became much rougher.

 doi:10.20944/preprints202406.0496.v1

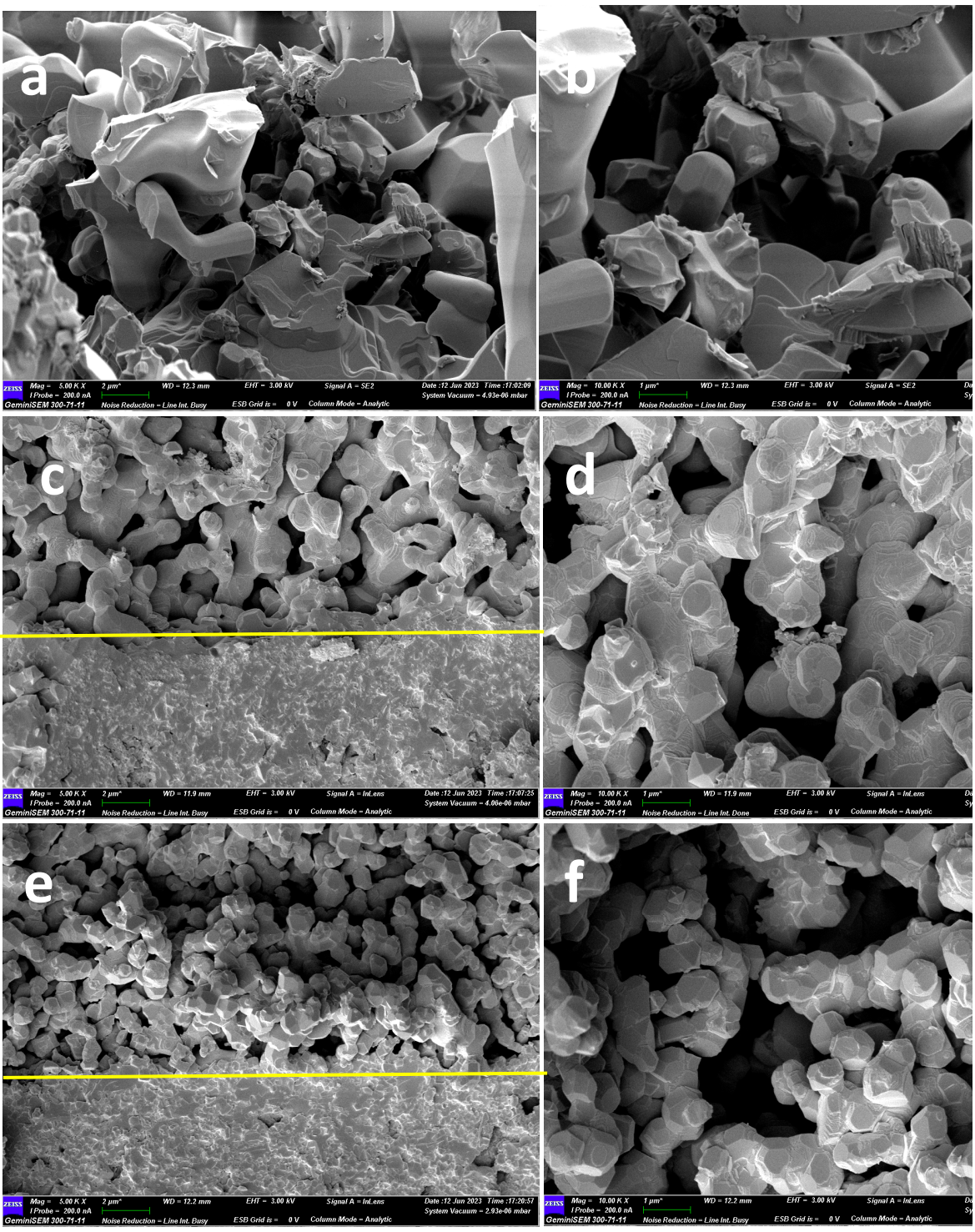

Figure 9. Cross-sectional micro structure of (a,b) LPBSCF3 cathode; (c,d) impregnated LPBSCF3-LN-0.04M cathode; (e,f) impregnated LPBSCF3-LN-0.08M cathode at a constant current density of 200 mA/cm^2 at 700 ^{o}C for 40 h in symmetrical cells.

Figure 10 shows the electrochemical performances of the LPBSCF3-LN-0.04M single button cell (NiO-YSZ|YSZ|GDC|LPBSCF3-LN-0.04M) at 800 °C. The OCV of the single cell closely matched theoretical values of 1.1 V, indicating the absence of cracks in the button cell, whereas the single cell with the LPBSCF3-LN-0.04M cathode demonstrated an MPD of 800 mW/cm^2. Moreover, Figure S1 shows the single-cell performance of LPBSCF3, indicating that the MPD was 743 mW/cm^2 at 800 °C, which was lower than that of the LPBSCF3-LN-0.04M single cell. The curving point of the I–V curve was presumably due to the button cell being in an activated state in the early stage when switching from low to high temperatures; however, after stable testing, a sudden change occurred. The tests

 doi:10.20944/preprints202406.0496.v1

were optimized in the next step. More importantly, the (NiO-YSZ|YSZ|GDC|LPBSCF3-LN-0.04M) cell showed excellent operating stability during the galvanostatic test at 800 °C for 100 h, as shown in Figure 11.

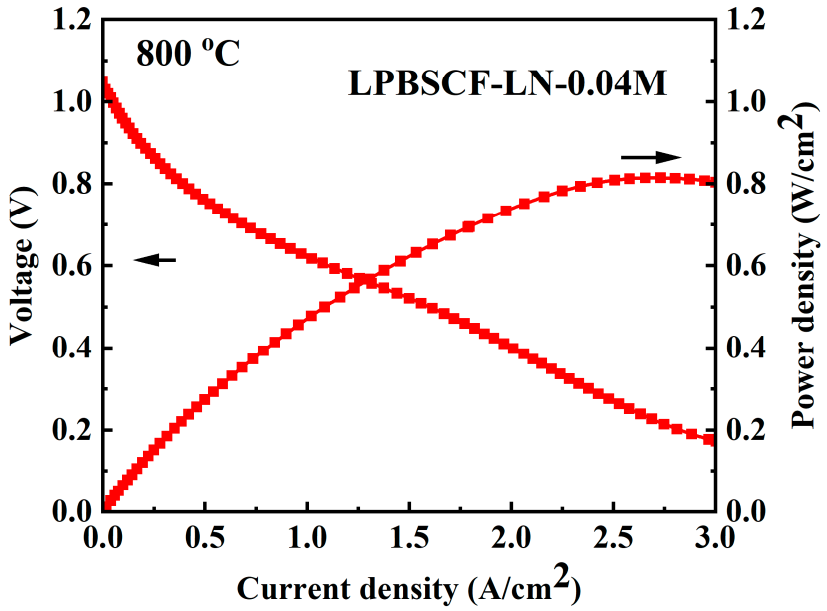

Figure 10. I-V-P curves of Ni-YSZ anode-supported single cells using impregnated LPBSCF3-LN-0.04M as the cathode at 800 °C.

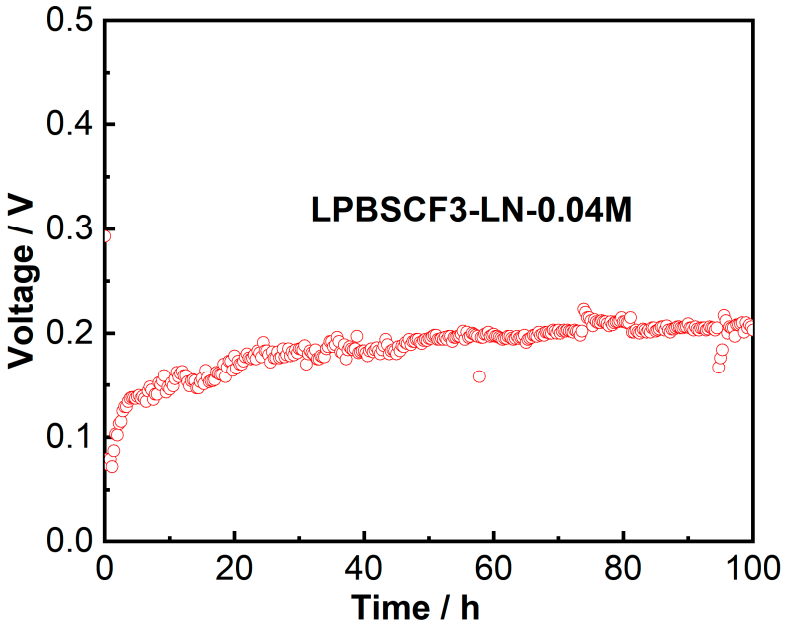

Figure 11. Stability test of impregnated LPBSCF3-LN-0.04M anode-supported single cells tested at a constant current density of 100 mA/cm² at 800 °C for 100 h.

 doi:10.20944/preprints202406.0496.v1

4. Conclusions

A series of double perovskite-type oxide $La_{1-x}Pr_xBa_{0.5}Sr_{0.5}Co_{1.5}Fe_{0.5}O_{5+\delta}$ (x=1,0.3,0) were synthesised using EDTA-CA as cathodes of IT-SOFC. LPBSCF(x=0.3) exhibited a pure cubic perovskite structure phase after sintering at 1000 °C for 3 h. An optimum impregnation amount of LN-LPBSCF (0.64 mg/cm²) electrodes exhibited lower Rp and better stable performance compared to that of pure LPBSCF electrode in symmetrical SOFC. Anode-supported YSZ-based SOFC with impregnated LPBSCF3-LN-0.04M cathode showed an MPD of 800 mW/cm² at 800 °C. Impregnated single cells also exhibited excellent operating stability at 800 °C for 100 h. These findings suggest that double perovskite oxides are promising materials for application in SOFC cathodes.

Acknowledgments: The authors acknowledge the facilities, the scientific and technical assistance of Hoffman Advanced Materials Research Institute from Shenzhen Polytechnic University. The authors also acknowledge the supports from 2023 National Natural Science Foundation of China (52302295), 2022 Shenzhen Science and Technology Program (GJHZ20210705142006020), 2022 Research Funding from Shenzhen Polytechnic (6022310007K), Sichuan science and technology program (2022YFH0044), the project of Civil Aviation Flight University of China (J2020-045), Sichuan Technology & Engineering Research Center for Vanadium Titanium Materials (2020FTGC-Z-05).

Conflicts of Interest: The authors declare that they have no known competing financial interests or personal relationships that could have appeared to influence the work reported in this paper.

References

1. Fergus, J.W., *Effect of cathode and electrolyte transport properties on chromium poisoning in solid oxide fuel cells.* International Journal of Hydrogen Energy, 2007. **32**: p. 3664-3671.
2. Horita, T., et al., *Effects of impurities on the degradation and long-term stability for solid oxide fuel cells.* Journal of Power Sources, 2009. **193**(1): p. 194-198.
3. Schuler, J.A., et al., *Air side contamination in Solid Oxide Fuel Cell stack testing.* Journal of Power Sources, 2011. **196**(17): p. 7225-7231.
4. Tu, H.Y. and U. Stimming, *Advances, aging mechanisms and lifetime in solid-oxide fuel cells.* Journal of Power Sources, 2004. **127**(1-2): p. 284-293.
5. Bello, I.T., et al., *Scientometric review of advancements in the development of high-performance cathode for low and intermediate temperature solid oxide fuel cells: Three decades in retrospect.* International Journal of Hydrogen Energy, 2021. **46**(52): p. 26518-26536.
6. Li, J., et al., *Novel gradient porous cathode for intermediate temperature solid oxide fuel cell.* International Journal of Hydrogen Energy, 2019. **44**(59): p. 31525-31530.
7. Chen, F., et al., *Doping strategy on improving the overall cathodic performance of double perovskite $LnBaCo_2O_{5+\delta}$ (Ln=Pr, Gd) as potential SOFC cathode materials.* Journal of Materiomics, 2023. **9**(5): p. 825-837.
8. Liu, Y., et al., *Novel CO_2-tolerant Co-based double perovskite cathode for intermediate temperature solid oxide fuel cells.* Journal of the European Ceramic Society, 2023. **43**(3): p. 1028-1038.
9. Grassi, J., et al., *Power density vs ionic radii correlations in $REBa_2Cu_3O_{6+\delta}$ (RE = La, Nd, Sm, Gd and Y) IT – SOFC potential cathodes.* Electrochimica Acta, 2023. **464**: p. 142931.
10. Bao, X., et al., *Effects of Bi-doping on structure and properties of $YBaCo_2O_{5+\delta}$ layered perovskite cathode for intermediate-temperature solid oxide fuel cells.* Journal of Alloys and Compounds, 2023. **965**: p. 171391.
11. Qian, B., et al., *Cobalt-free double-perovskite oxide $Sr_2Ti_{0.9}FeNi_{0.1}O_6$ as a promising electrode for symmetric solid oxide electrolysis cells.* Journal of the European Ceramic Society, 2023.
12. Wang, S., et al., *Evaluation of perovskite oxides $LnBaCo_2O_{5+\delta}$ (Ln = La, Pr, Nd and Sm) as cathode materials for IT-SOFC.* Journal of Electroanalytical Chemistry, 2021. **886**: p. 115144.
13. Wang, H., et al., *Exploring the influence of rare earth ions at A-site on the properties of $LnBaCo_2O_{5+\delta}$ cathode for solid oxide fuel cells.* Ceramics International, 2023. **49**(16): p. 27222-27229.
14. Dou, Y., et al., *Addressing electrocatalytic activity and stability of $LLnBaCo_2O_{5+\delta}$ perovskites for hydrogen evolution reaction by structural and electronic features.* Applied Catalysis B: Environmental, 2021. **297**: p. 120403.
15. Chen, D.J., R. Ran, and Z.P. Shao, *Assessment of $PrBaCo_2O_{5+\delta}$ + $Sm_{0.2}Ce_{0.8}O_{1.9}$ composites prepared by physical mixing as electrodes of solid oxide fuel cells.* JOURNAL OF POWER SOURCES, 2010. **195**(21): p. 7187-7195.
16. Wang, H.R., et al., *A novel composite oxygen electrode: $PrBaCo_2O_{5+\delta}$ combined with negative thermal expansion oxide applied to reversible solid oxide cells.* INTERNATIONAL JOURNAL OF HYDROGEN ENERGY, 2022. **47**(90): p. 38327-38333.
17. Bai, H., et al., *$PrBa_{0.5}Sr_{0.5}Co_{1.5}Fe_{0.5}O_{5+\delta}$ as air electrode for proton-conducting solid oxide cells.* JOURNAL OF POWER SOURCES, 2023. **574**.

 doi:10.20944/preprints202406.0496.v1

18. Jiang, S.P., *Nanoscale and nano-structured electrodes of solid oxide fuel cells by infiltration: Advances and challenges.* International Journal of Hydrogen Energy, 2012. **37**(1): p. 449-470.
19. Ai, N., et al., *Nanostructured (Ba,Sr)(Co,Fe)$O_{3-\delta}$ Impregnated (La,Sr)MnO_3 Cathode for Intermediate-Temperature Solid Oxide Fuel Cells.* Journal of the Electrochemical Society, 2010. **157**(7): p. B1033-B1039.
20. Chen, J., et al., *Palladium and ceria infiltrated $La_{0.8}Sr_{0.2}Co_{0.5}Fe_{0.5}O_{3-\delta}$ cathodes of solid oxide fuel cells.* Journal of Power Sources, 2009. **194**(1): p. 275-280.
21. He, H.Q., et al., *Co_2MnO_4 spinel-palladium co-infiltrated $La_{0.7}Ca_{0.3}Cr_{0.5}Mn_{0.5}O_{3-\delta}$cathodes for intermediate temperature solid oxide fuel cells.* Journal of Alloys and Compounds, 2011. **509**(40): p. 9708-9717.
22. Jiang, S.P., *A review of wet impregnation - An alternative method for the fabrication of high performance and nano-structured electrodes of solid oxide fuel cells.* Materials Science and Engineering a-Structural Materials Properties Microstructure and Processing, 2006. **418**(1-2): p. 199-210.
23. Jiang, S.P. and W. Wang, *Fabrication and performance of GDC-impregnated (La,Sr)MnO_3 cathodes for intermediate temperature solid oxide fuel cells.* Journal of the Electrochemical Society, 2005. **152**(7): p. A1398-A1408.
24. Liang, F., et al., *Novel nano-structured Pd plus yttrium doped ZrO_2 cathodes for intermediate temperature solid oxide fuel cells.* Electrochemistry Communications, 2008. **10**(1): p. 42-46.
25. Liang, F., et al., *Development of Nanostructured and Palladium Promoted (La,Sr)$MnO_{(3)}$-Based Cathodes for Intermediate-Temperature SOFCs.* Electrochemical and Solid State Letters, 2008. **11**(12): p. B213-B216.
26. Zhao, L., S. Amarasinghe, and S.P. Jiang, *Enhanced chromium tolerance of $La_{0.6}Sr_{0.4}Co_{0.2}Fe_{0.8}O_{3-\delta)}$ electrode of solid oxide fuel cells by $Gd_{0.1}Ce_{0.9}O_{1.95}$ impregnation.* Electrochemistry Communications, 2013. **37**: p. 84-87.
27. Chen, K., et al., *Highly chromium contaminant tolerant BaO infiltrated $La_{0.6}Sr_{0.4}Co_{0.2}Fe_{0.8}O_{3-\delta}$ cathodes for solid oxide fuel cells.* Physical Chemistry Chemical Physics, 2015. **17**(7): p. 4870-4874.
28. Huang, J., et al., *Promotional role of $BaCO_3$ on the chromium–tolerance of $La_{0.6}Sr_{0.4}Co_{0.2}Fe_{0.8}O_{3-\delta}$ cathodes of solid oxide fuel cells.* Applied Catalysis B: Environmental, 2023. **321**: p. 122080.
29. Jiang, L., et al., *Thermal and electrochemical properties of $PrBa_{0.5}Sr_{0.5}Co_{2-x}Fe_xO_{5+\delta}$ (x = 0.5, 1.0, 1.5) cathode materials for solid-oxide fuel cells.* Journal of Power Sources, 2013. **232**: p. 279-285.
30. Zhang, X., H. Zhang, and X. Liu, *High performance $La_2NiO_{4+\delta}$-infiltrated $(La_{0.6}Sr_{0.4})_{0.995}Co_{0.2}Fe_{0.8}O_{3-\delta}$ cathode for solid oxide fuel cells.* Journal of Power Sources, 2014. **269**: p. 412-417.
31. Wei, M., et al., *High performance $La_2NiO_{4+\delta}$ impregnated $(La_{0.6}Sr_{0.4})_{0.995}Co_{0.2}Fe_{0.8}O_{3-\delta}$ cathodes for solid oxide fuel cells.* Solid State Ionics, 2022. **387**: p. 116065.
32. Li, J., et al., *Microstructure optimization for high-performance $PrBa_{0.5}Sr_{0.5}Co_{1.5}Fe_{0.5}O_{5+\delta}$-$La_2NiO_{4+\delta}$ i core-shell cathode of solid oxide fuel cells.* Journal of Power Sources, 2018. **379**: p. 206-211.